

Sufficient noise and turbulence can induce phytoplankton patchiness

Hiroshi Serizawa¹, Takashi Amemiya², Kiminori Itoh¹

¹ Graduate School of Engineering, Yokohama National University, Yokohama, Japan; seri@qb3.so-net.ne.jp; itohkimi@ynu.ac.jp

² Graduate School of Environment and Information Sciences, Yokohama National University, Yokohama, Japan; amemiya@ynu.ac.jp

Received 25 November 2009; revised 28 December 2009; accepted 3 February 2010.

ABSTRACT

Phytoplankton patchiness ubiquitously observed in marine ecosystems is a simple physical phenomenon. Only two factors are required for its formation: one is persistent variations of inhomogeneous distributions in the phytoplankton population and the other is turbulent stirring by eddies. It is not necessary to assume continuous oscillations such as limit cycles for realization of the first factor. Instead, a certain amount of noise is enough. Random fluctuations by environmental noise and turbulent advection by eddies seem to be common in open oceans. Based on these hypotheses, we propose seemingly the simplest method to simulate patchiness formation that can create realistic images. Sufficient noise and turbulence can induce patchiness formation even though the system lies on the stable equilibrium conditions. We tentatively adopt the two-component model with nutrients and phytoplankton, however, the choice of the mathematical model is not essential. The simulation method proposed in this study can be applied to whatever model with stable equilibrium states including one-component ones.

Keywords: Eddy; Fluctuation; Noise; Patchiness; Reaction-Advection-Diffusion Model; Turbulence

1. INTRODUCTION

Patchiness is the inhomogeneous distribution of phytoplankton observed all over the oceans from the tropic to the boreal zone (Figure 1). The characteristic pattern with stretched and curled structures appears in the mesoscale or sub-mesoscale region from one to hundreds of kilometers, where the surface flow is approximately two-dimensional, *i.e.*, horizontal [1]. This obser-

vation suggests that the main cause of the phenomenon is referred to the physical factors such as lateral turbulent stirring and mixing by currents and eddies.

It is well known that the spatially inhomogeneous patterns can be generated in reaction-diffusion or reaction-advection-diffusion systems with equal diffusivities. One of the remarkable studies using reaction-diffusion equations was conducted by Medvinsky *et al.* [2]. They demonstrated that the diffusive instability can lead the system to spatiotemporal chaos even though starting from simple initial conditions. However, the chaotic patterns arising from reaction-diffusion systems do not necessarily mimic the real phytoplankton patchiness as seen in Figure 1. Without advection terms, stretched and curled structures characteristic of marine patchiness are not properly reproduced.

The situation is much improved by incorporating the effects of advection into the model. The simulation images created by reaction-advection-diffusion systems seem to show a closer similarity to real patchiness patterns than those by reaction-diffusion systems [3-6]. The studies by reaction-advection-diffusion systems usually adopt the seeded-eddy model to represent two-dimensional turbulent flows, which is developed by Dyke and Robertson [7].

However, the controversy is that the above mentioned studies using reaction-diffusion or reaction-advection-diffusion equations assume the limit cycle oscillations as the origin of heterogeneity in phytoplankton distributions. Considering that the system with the stable equilibrium state is meant to be homogeneous even though the initial state is heterogeneous [8], any pattern formation seems to require some kind of mechanisms such as limit cycles that continue to oscillate the system. However, it is not clear whether the limit cycle oscillations are usual events in natural aquatic ecosystems. Limit cycle oscillations could be too severe for the precondition of patchiness formation. To avoid the contradiction, it is necessary to seek the alternative mechanism other than the limit cycle oscillation.

One of the candidates that can replace the limit cycle oscillation could be persistent noise, which also can provide continuous changes of phytoplankton population.

Recently, Vainstein *et al.* [9] examined the stochastic population dynamics in the turbulent field, using a two-component reaction-advection-diffusion model with phytoplankton and zooplankton. In their model, the equation of zooplankton only contains the noise term for the reason that the population of zooplankton is considerably smaller than that of phytoplankton and thus subject to stochastic processes. The zooplankton distribution shows the finer structure than the phytoplankton distribution in their simulations, which is consistent with field observations. However, the phytoplankton distribution reproduced by their model does not seem to resemble real satellite images such as **Figure 1**.

Ecological systems are open systems in which the interactions with the external environment are noisy [10,11]. Thus, it is natural to incorporate random fluctuations into the model. However, proper incorporation of noise is not easy. For example, there are mathematically two types of noise: one is the additive noise and the other is the multiplicative noise [12]. The multiplicative noise is dependent on the dynamical variables, while the additive noise is independent of them. The multiplicative noise is thought to be caused by the interaction between the corresponding component and the external environment [10,13]. However, clear criteria do not necessarily exist for which type of noise should be used in a given situation. The decision rests more or less on the individual modeler.

The technical problem in computer simulations is more crucial. The stochastic spatiotemporal simulations of the partial differential equation model are strongly affected by such factors as the spatial correlation length and the temporal frequency of random noise. Therefore, it is important to determine appropriate values for these parameters in order that the effects of noise are properly reflected to simulation processes. In particular, the temporal frequency of noise is subtle to be handled. If the changing speed of noise is too fast or the period of subsequent noise is too short, successful pattern formation cannot be expected.

The goal of this paper is to specify the ultimate causes for patchiness formation and to propose a simple and convenient simulation method for its reproduction. We construct the model on the basis of the same concept as that by Vainstein *et al.* [9]. That is, the model includes the effect of temporally fluctuating noise as well as those of diffusion and advection. However, the substantial difference lies on the way to incorporate noise into the model. The simulation images obtained by our method seem to show a striking resemblance to real patchiness patterns as seen in **Figure 1**.

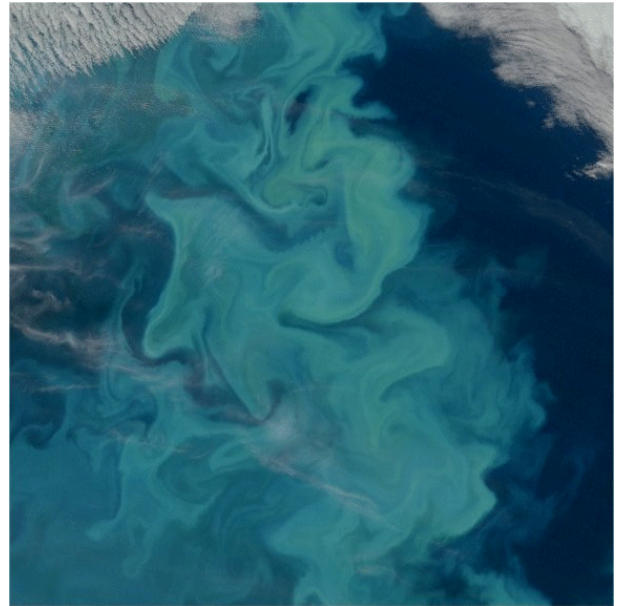


Figure 1. Algal blooms in the Barents Sea (Credit: NASA Goddard Space Flight Center).

Our two-component model consists of nutrients and phytoplankton. However, the model itself is not essential. The simulation method used in this study is not only effective for a wide range of parameter settings but also applicable to other mathematical models. Robustness and applicability could afford considerable credibility to our method.

2. MATHEMATICAL MODEL

2.1. Mean-Field Model

First, we present the mean-field model that describes the biological interaction. The ordinary differential equations are given as follows:

$$\frac{dN}{dt} = I_N - k\mu \frac{N}{H_N + N} P - m_N N, \quad (1)$$

$$\frac{dP}{dt} = I_P + \mu \frac{N}{H_N + N} P - f_P \frac{P}{H_P + P} - m_P P. \quad (2)$$

Two state variables N and P represent the nutrient concentration (the unit is mmol/m^3) and the phytoplankton density (the unit is g/m^3), respectively. The other variable t is actual time (the unit is day). With regard to the parameters, I_N and I_P are the input rates of nutrients and phytoplankton from the external environment, μ is the maximum growth rate of phytoplankton, k is the nutrient content in phytoplankton, f_P is the maximum predation rate of zooplankton on phytoplankton, m_N is the removal rate of nutrients from the system, m_P is the natural mortality rate of phytoplankton, and H_N and H_P are the half-saturation constants of nutrients and phyto-

Table 1. Parameters in minimal NP models **Eqs.1** and **2** and **Eqs.7-9**.

Parameters	Meanings	Set I	Set II	Units
I_N	Input rate of nutrients	0.4	0.15	$\text{mmol} \cdot \text{m}^{-3} \cdot \text{day}^{-1}$
k	Nutrient content in phytoplankton	0.2	0.2	mmol/g
H_N	Half-saturation constant of nutrients	0.2	0.2	mmol/m^3
m_N	Removal rate of nutrients	0.1	0.02	day^{-1}
I_P	Input rate of phytoplankton	0.04	0.04	$\text{g} \cdot \text{m}^{-3} \cdot \text{day}^{-1}$
μ	Maximum growth rate of phytoplankton	0.5	0.5	day^{-1}
f_P	Maximum feeding rate of zooplankton on phytoplankton	2.0	2.0	$\text{g} \cdot \text{m}^{-3} \cdot \text{day}^{-1}$
H_P	Half-saturation constant of phytoplankton	4.0	4.0	g/m^3
m_P	Mortality rate of phytoplankton	0.1	0.1	day^{-1}
D	Diffusion coefficient	0.125	0.125	km^2/day
r_c	Radius of eddies	10.0 (20.0)	10.0	km
V_{max}	Maximum velocity	10.0 (10.0)	10.0	km/day
V_{av}	Average velocity	2.98 (3.50)	2.98	km/day
L	Half length of square domain side	100	100	km

The Set I is used for the simulations in **Figures 5, 6** and **7**, while the Set II is used in **Figure 8**. The values within parentheses in the Set I correspond to the VF I in **Figure 2(a)**, which is used only for the simulation in **Figure 6(a)**.

plankton, respectively. The mathematical model **Eqs.1** and **2**, named the minimal NP model in the present study, is known to show both bistability and limit cycle oscillations for the parameter values within the realistic range [6,8]. The meanings and the units of these parameters are listed in **Table 1** together with their values.

It is worth pointing out that the input term of phytoplankton I_P and the removal term of nutrients $m_N N$ contribute to stabilizing the system. For example, the situation that the phytoplankton density $P = 0$, where phytoplankton continue to be extinct, can be avoided by the parameter I_P . Moreover, even if $P = 0$, the other unfavorable situation that the nutrient concentration N continues to increase unlimitedly can be avoided by the term $m_N N$.

2.2. Velocity Field

Turbulent stirring is considered to be a crucial factor in creating phytoplankton patchiness in marine ecosystems. In this study, we use a simplified version of the seeded-eddy model as two-dimensional turbulent flows [3,6,7,9,14]. The stream function ψ and fluid velocity V are described as follows:

$$\psi(x, y) = A \sum_i \sigma_i r_i^2 \exp\left\{-\frac{(x-x_i)^2 + (y-y_i)^2}{2r_i^2}\right\}, \quad (3)$$

$$\sigma_i = 1 \text{ or } -1, \quad V = (V_x, V_y) = \left(-\frac{\partial \psi}{\partial y}, \frac{\partial \psi}{\partial x}\right).$$

Suppose that the number of eddies is denoted by n . Then, the velocity field is composed of n eddies, the half of which rotate clockwise, while the other half rotate counter-clockwise. The center of each eddy (x_i, y_i) is randomly dispersed within the domain. For simplicity, we use a constant value of the radius r_i for all eddies without considering a distribution of variant eddy sizes. Thus, $r_i = r_c$ (constant). It is supposed that the velocity field is mainly composed by eddies with larger radii, because the stream function ψ is proportional to the square of the radius r_i^2 . The use of the constant radius can be justified for this reason. In fact, no essential difference is observed in the final appearance of patchiness patterns as compared to the case in which the eddy sizes are varied. The adoption of the constant radius is for the sake of speedy simulations. The scaling constant A is introduced for the adjustment of the maximum velocity V_{max} .

Figure 2 shows the velocity fields V used in the present study. The number and the radius of eddies are $n = 40$ and $r_c = 20$ km in **Figure 2(a)**, while $n = 100$ and $r_c = 10$ km in **Figure 2(b)**. The former velocity field is referred to as the VF I, and the latter is as the VF II. In most of the simulations except for **Figure 6(a)**, the VF II is employed. The domain is a $200 \text{ km} \times 200 \text{ km}$ square, that is, a half length of each side is $L = 100$ km. The maximum velocity V_{max} is set up at 10 km/day for both velocity fields by varying the scaling parameter A . Then,

the average velocities become 3.50 km/day in the VF I, while 2.98 km/day in the VF II. Both velocity fields are stationary and remain temporally unchanged, and also meet the periodic boundary conditions.

2.3. White Noise Process

Random fluctuations are constructed as explained in our previous study [8]. First, we provide a fluctuation function to describe a spatially smoothed deviation. The fluctuation function is formulated using the following Gaussian distribution function:

$$G_{x_i, y_i}(x, y) = \exp\left\{-\frac{(x-x_i)^2 + (y-y_i)^2}{2s^2}\right\} \quad (4)$$

The function G depicts a convex curved surface whose peak locates at (x_i, y_i) , and the peak value equals 1. Here, the parameter s denotes the correlation length of fluctuations. The convex Gaussian function G is named the plus-type, and we can also formulate the minus-type Gaussian function, denoted as $-G$, that creates a concave valley.

Thereafter, a total of 100 Gaussian functions are provided with different (x_i, y_i) values, which consist of 50 plus-type ones and 50 minus-type ones. As the location of the peak or the valley (x_i, y_i) is randomly dispersed within the domain, the unevenly waved surface can be generated by the superposition of these Gaussian functions, the average height of which equals 0. Then, the fluctuation function F is defined as follows:

$$F(x, y) = \sum_i \sigma_i G_{x_i, y_i}(x, y), \quad \sigma_i = 1 \text{ or } -1. \quad (5)$$

The position coordinates of peaks and valleys (x_i, y_i) are different depending on the index i .

Assuming that the peak position (x_i, y_i) is a function of time t , the fluctuation function F is also a function of t , thus, $F(x, y, t)$. Then, we can use the function $F(x, y, t)$ as time-dependent fluctuations $\delta_{N,P}(x, y, t)$ for both the nutrient concentration N and the phytoplankton density P according to the following equation:

$$\delta_{N,P}(x, y, t) = A_{N,P} F(x, y, t). \quad (6)$$

Here, the parameter A_N and A_P denote the scale factors of fluctuations for nutrients and phytoplankton. The functions $\delta_{N,P}(x, y, t)$ are referred to as the noise distribution function in this study. For example, the noise distributions for phytoplankton by $\delta_P(x, y, t)$ are shown in **Figure 3** for three elapsed time, where **Figure 3(a)** is the initial distribution of $\delta_P(x, y, t)$ when $t = 0$. The noise distribution function $\delta_P(x, y, t)$ continues to change alike, thereafter, and $\delta_N(x, y, t)$ changes as well.

2.4. Reaction-Advection-Diffusion Model

Finally, we construct the reaction-advection-diffusion model that synthesizes the above-mentioned factors, that

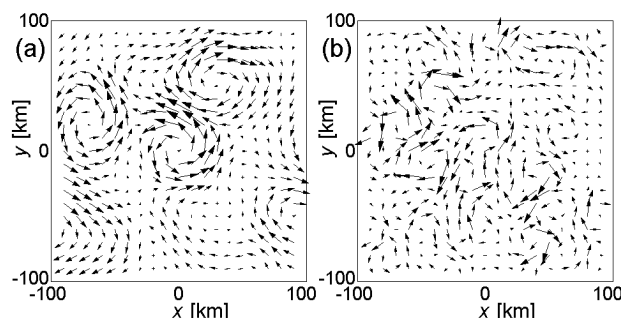


Figure 2. Velocity fields by turbulent stirring. The velocity field is constructed by the superimposition of n eddies with the constant radius r_c . (a) $n = 40, r_c = 20$ km. (b) $n = 100, r_c = 10$ km. These are named the VF I and the VF II, respectively. The velocity fields meet the periodic boundary conditions.

is, the biological interaction, turbulence and noise. Using the right side of the **Eqs.1** and **2**, we can formulate the following two-dimensional reaction-advection-diffusion model:

$$\frac{\partial N}{\partial t} = D\nabla^2 N - \nabla \cdot (VN) + I_N - k\mu \frac{N}{H_N + N} P - m_N N + N\delta_N(x, y, t), \quad (7)$$

$$\frac{\partial P}{\partial t} = D\nabla^2 P - \nabla \cdot (VP) + I_P + \mu \frac{N}{H_N + N} P - f_P \frac{P}{H_P + P} - m_P P + P\delta_P(x, y, t). \quad (8)$$

The Laplacian operators are described as follows:

$$\nabla = \left(\frac{\partial}{\partial x}, \frac{\partial}{\partial y} \right), \quad \nabla^2 = \frac{\partial^2}{\partial x^2} + \frac{\partial^2}{\partial y^2}. \quad (9)$$

The variables x and y are the horizontal position coordinates (the unit is km). The parameter D denotes the lateral diffusivity, which is equal for two components. Further, the vector V represents the velocity field shown in **Figure 2**. It should be noted that the units of state variables N and P are changed to mmol/m² and g/m² due to the adoption of the two-dimensional model.

As stated previously, there are two types of noise, the additive noise and the multiplicative noise. The mathematical model **Eqs.7-9** contains the stochastic fluctuation terms in the right-hand sides of the partial differential equations, which are described in the multiplicative forms as $+N\delta_N(x, y, t)$ for nutrients and $+P\delta_P(x, y, t)$ for phytoplankton. This is because we assume the interactions with the external environment for both nutrients and phytoplankton. However, even if the additive noise is added for both components, the results are hardly affected. Thus, which type of noise is used is not essential in the current study. What is important is to set the amplitude of noise within adequate values by adjusting the scale parameters A_N and A_P in order to avoid the situation

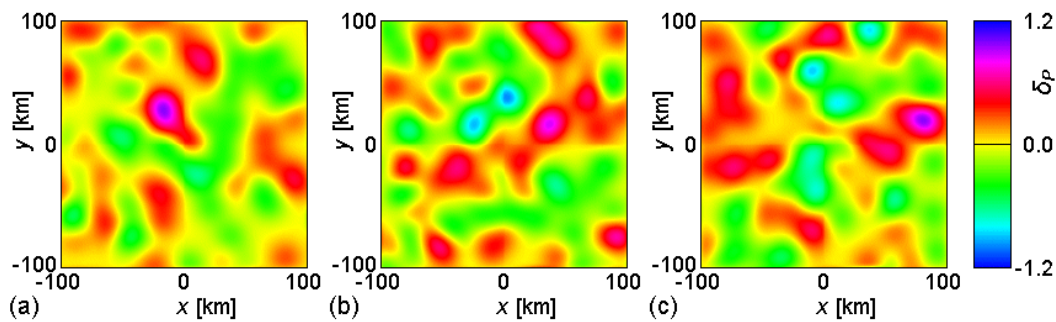


Figure 3. Spatiotemporal variation of noise distribution for phytoplankton. The distribution of noise for the phytoplankton density P is represented by the noise distribution function $\delta_P(x, y, t)$. (a) shows the initial distribution $\delta_P(x, y, 0)$, which is changed to (b) and (c) consecutively. The noise distributions also meet the periodic boundary conditions.

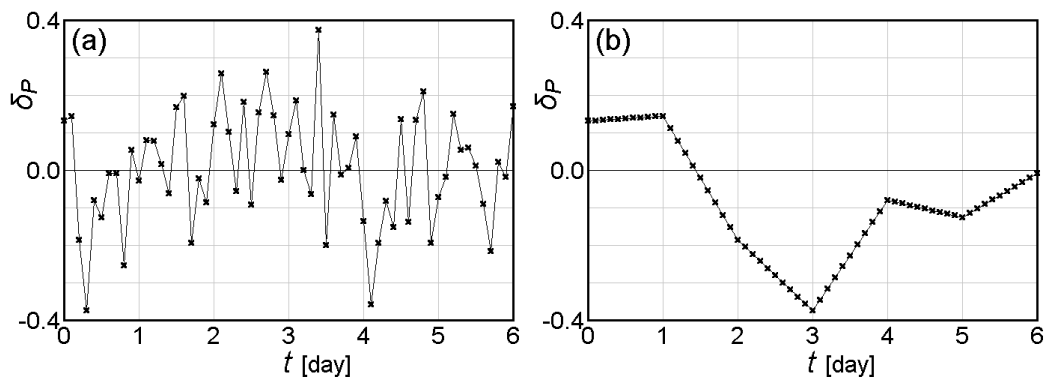


Figure 4. White noise processes at $(0, 0)$. These line graphs show the temporal change of the noise distribution function $\delta_P(x, y, t)$ for phytoplankton at the center of the domain, *i.e.*, $\delta_P(0, 0, t)$. The time step of the simulations $\Delta t = 0.1$ day, meaning that the calculation is carried out 10 times a unit time, which equals a day. Renewed noise distribution functions are provided every time step in (a) and every 10 time steps, *i.e.*, everyday in (b), respectively. Also in (b), the amplitude of noise is changed linearly at each time step between two days. The white noise processes described in (a) and (b) are named the WN I and the WN II, respectively.

that the population of the component falls to the negative values.

In white noise processes, the amplitude of the fluctuation, *i.e.*, deviation from the mean value is randomly distributed within a certain range at each cell and each unit time. If the difference of the amplitude between adjacent cells or subsequent time steps is too large, the system is often led to divergence.

The temporal change of fluctuations is determined as follows. According to the noise distribution functions $\delta_{N,P}(x, y, t)$, the amplitudes of fluctuations for both nutrients and phytoplankton change independently at each cell. Assuming that the time step of the simulation $\Delta t = 0.1$ day, the calculations are conducted ten times a unit time, *i.e.*, a day. Further, the noise distribution functions $\delta_{N,P}(x, y, t)$ are renewed every time step (**Figure 4(a)**) or every ten time steps (**Figure 4(b)**). In the latter case, the renewal of $\delta_{N,P}(x, y, t)$ is performed every unit time, *i.e.*, everyday, and the amplitude of fluctuations

varies linearly between successive two distributions. The temporal change of random noise for the phytoplankton density P at the center of the domain $\delta_P(0, 0, t)$ is depicted in **Figure 4** for these two cases, which are referred to as the WN I and the WN II, respectively. The WN I is used only for the simulation in **Figure 7(a)**. Otherwise, the WN II is employed.

In our spatiotemporal simulations, the domain is a $200 \text{ km} \times 200 \text{ km}$ square, and a half length of each side $L = 100 \text{ km}$. Then, the two-dimensional square domain is divided into a rectangular grid of 200×200 cells. Therefore, each cell is a $1.0 \text{ km} \times 1.0 \text{ km}$ square, and the noise distribution functions $\delta_{N,P}(x, y, t)$ are allocated to each cell. In the initial state, the distribution of both components are homogeneous, however, inhomogeneous distributions are realized just after the onset of simulations due to random fluctuations. The fourth order Runge-Kutta integrating method is applied with a time step $\Delta t = 0.1$ day, and the periodic boundary conditions are imposed.

It is confirmed that the results with smaller time steps remain the same for each program, ensuring the accuracy of the simulations.

3. RESULTS

3.1. Simulations with Noise (Set I)

Prior to spatiotemporal simulations of the reaction-advection-diffusion model **Eqs.7-9**, we conduct the stability analyses of the mean-field model **Eqs.1 and 2**. The results are shown in **Table 2**. For the parameter Set I in **Table 1**, the systems **Eqs.1 and 2** have only one fixed point. As the real parts of two eigenvalues are both negative, this fixed point is identified as an attractor that represents the stable equilibrium state. Therefore, even if the initial state is heterogeneous, the system is damped out to the uniform distribution in the course of time without continuous fluctuations.

Figure 5 shows the spatiotemporal variation of phytoplankton density P for the parameter Set I, in which the effects of turbulence and noise are both considered. The VF II given by **Figure 2(b)** and the WN II described in **Figure 4(b)** are applied for the simulations. While the initial state is homogeneous, the spatial distribution of phytoplankton begins to be disturbed soon due to the combined effects of furious turbulence and random noise. Then, as early as the ninth day, patchiness formation is perfectly completed, and continues to change, thereafter. It should be noted that the same pattern does not occur again, because the stochastic perturbation is not periodic.

Table 2. Stability analyses in minimal NP model **Eqs.1 and 2**.

	Set I	Set II
(N_0, P_0)	(0.259, 6.631)	(1.656, 1.31)
Eigenvalues	$-0.309 \pm 0.029i$	$0.017 \pm 0.037i$
Stability	Stable	Unstable
State	Convergence	Limit cycle

The minimal NP model **Eqs.1 and 2** generates only one fixed point (N_0, P_0) for both Sets I and II within the region $N_0 > 0$ and $P_0 > 0$, showing the convergence for the Set I and the limit cycle oscillation for the Set II, respectively.

The dependence of the patchiness pattern on the turbulence fields are examined in **Figure 6**. The velocity fields used in **Figure 6(a)** and **(b)** are the VF I and the VF II in **Figure 2**, respectively. The broadly extended structures observed in **Figure 6(a)** are probably due to the mildness of currents in the VF I. In contrast, the stormy velocity field such as the VF II seems to generate the patchiness pattern with fine structures as seen in **Figure 6(b)**, showing a clear resemblance with real satellite images such as **Figure 1**.

Meanwhile, the dependence on the noise processes is investigated in **Figure 7**. The white noise processes corresponding to **Figures 7(a)** and **7(b)** are the WN I and the WN II in **Figure 4**, respectively. Too frequent change in the noise distributions could obscure the patchiness pattern as seen in **Figure 7(a)**. On the contrary, the patchiness image in **Figure 7(b)** shows a clear difference in phytoplankton density. Slowly changing fluctuations

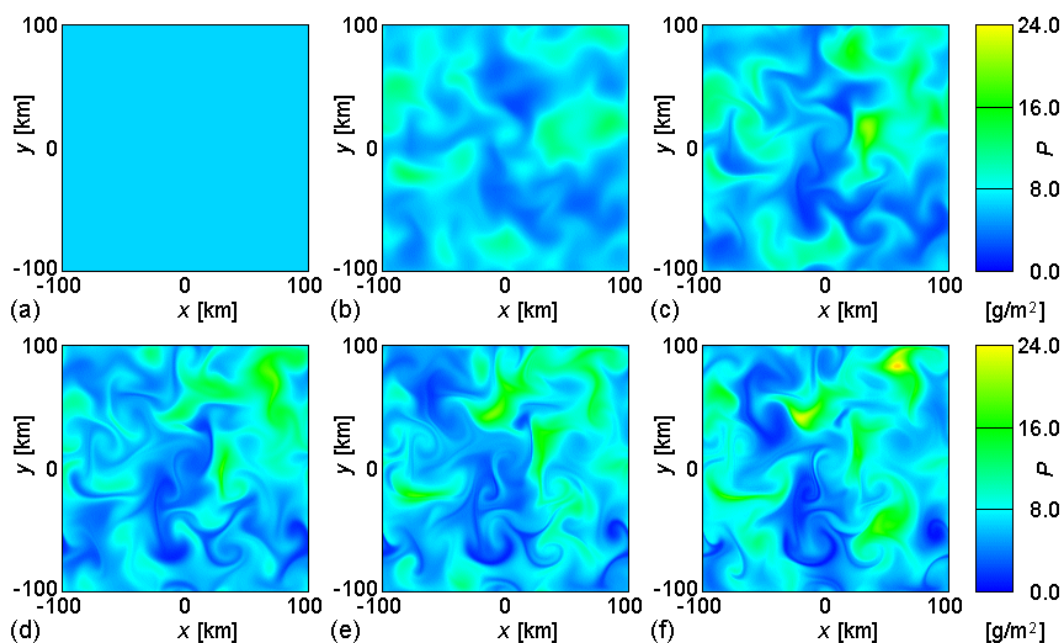


Figure 5. Spatiotemporal variation of phytoplankton distribution in minimal NP model **Eqs.7-9**. Without noise, the system shows a convergence to a stable equilibrium state for the parameter Set I in **Table 1**. However, incorporating random fluctuations into the model, patchiness formation is induced by the combined effects of turbulence and noise. The VF II and the WN II are employed. (a) $t = 0$ day, (b) $t = 3$ day, (c) $t = 6$ day, (d) $t = 9$ day, (e) $t = 12$ day, (f) $t = 15$ day.

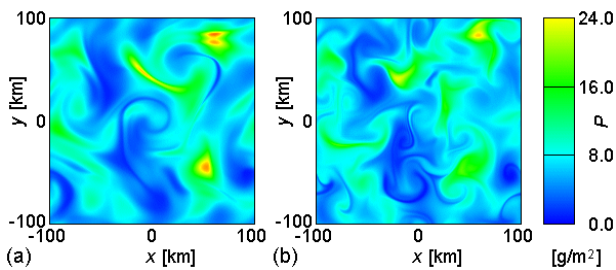


Figure 6. Dependence of phytoplankton distribution on velocity field in minimal NP model **Eqs.7-9**. The parameters are given by the Set I, and the WN II is employed. $t = 15$ day. (a) VF I, (b) VF II (same as **Figure 5(f)**).

intensify the effects of random noise, facilitating the emergence of both the densely populated and the sparsely populated areas.

3.2. Simulations with Limit Cycle Oscillation (Set II)

For the comparison, we also survey the pattern formation in the oscillatory regime. According to the stability analysis for the parameter Set II, the fixed point of the system becomes unstable as shown in **Table 2**, and the limit cycle is formed around it. In this case, random noise is not necessary, because the continuous oscillation encourages the pattern formation unless the initial distribution is homogeneous [6].

The spatiotemporal variation of phytoplankton density P for the parameter Set II is shown in **Figure 8**. Only the effect of turbulence is considered employing the VF II. Instead, the initial distributions of both components are not homogeneous but randomly dispersed. Patchiness patterns are formed also in this case for the almost same period as in **Figure 5**. However, it could be happened that the similar patterns appear repeatedly with the period of the limit cycle oscillation, which was the case in our previous study [6].

4. DISCUSSIONS

4.1. Comparison with Field Observations

Our simulation results seem to show a close similarity with satellite images such as **Figure 1**. Stretched and curled patterns characteristic of marine patchiness are clearly reproduced particularly in **Figure 5**, which employs energetic turbulence as the VF II and slowly changing white noise process as the WN II.

We attempt some kinds of numerical comparisons. First, the size of our simulation images are comparable to that of the satellite images in **Figure 1**, which covers the area of some hundreds kilometers. Considering that

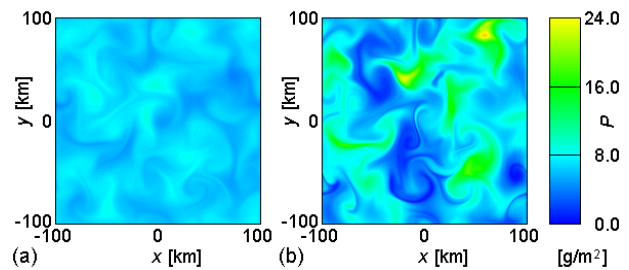


Figure 7. Dependence of phytoplankton distribution on white noise process in minimal NP model **Eqs.7-9**. The parameters are given by the Set I, and the VF II is employed. $t = 15$ day. (a) WN I, (b) WN II (same as **Figure 5(f)**).

most of the patchiness images supplied by NASA are of a similar size with **Figure 1**, we can insist that the velocity field and the noise process adopted in our method are suitable for patchiness simulations.

Comparing the horizontal diffusivity to experimental data, two types of diffusion must be distinguished [6,14]. The first type of diffusion is usual diffusion originating from a tendency toward homogeneity. This type of diffusion is represented by the second order differential for position coordinates. Thus, the diffusion coefficient D used in the minimal NP model **Eq.7-Eq.9** corresponds to this type. However, this type of diffusion does not stand for real diffusion in marine ecosystems. In the context of computer simulations, diffusion of this type merely functions as a smoothing factor that prevents divergence of the system.

Meanwhile, there exists another type of diffusion originating from advection by currents and eddies, which is represented by the first order differential for position coordinates. It is this type of diffusion that is responsible for patchiness formation in oceanic environments. Thus, the real diffusion coefficient must be recalculated from the velocity fields V in **Figure 2**.

The real diffusion coefficient D_{ad} can be evaluated by the following equation:

$$D_{ad} = \mu L_D^2. \quad (10)$$

As a rough approximation, suppose that the characteristic scale of diffusion L_D is given by the average velocity V_{av} . In the case the VF II in **Figure 2(b)** is $L_D \sim 3.0$ km. Then, we can estimate the value of turbulent diffusivity D_{ad} as about $4.5 \text{ km}^2/\text{day}$. This value is converted to about $5 \times 10^5 \text{ cm}^2/\text{sec}$, which is in agreement with the empirical data estimated by Okubo [15] that range from 5×10^2 to $2 \times 10^6 \text{ cm}^2/\text{sec}$.

4.2. Crucial Factors for Patchiness Formation

Turbulence and persistent variation of phytoplankton population are two essential factors for creating marine patchiness. Particularly as for turbulence, many re-

searchers take it for granted that lateral advection and mixing by currents and eddies plays a constructive role for patchiness formation [1]. However, there seems to be no consensus for another factor at the present time. According to our simulations, both random noise and limit cycle oscillations can cause persistent variation, and promote patchiness formation as shown in **Figures 5** and **8**. It is not yet clear about which is the ultimate cause for persistent variation of phytoplankton population. Which is more probable as a crucial factor in patchiness formation, noise or limit cycles? It seems difficult to judge from the appearance of simulation images.

Becks *et al.* [16] reported that a defined chemostat system with bacteria and ciliate showed dynamic behaviors such as chaos and stable limit cycles. In their two-prey, one-predator system, the changes of the bifurcation parameter (the dilution rate) trigger the population dynamics such as stable coexistence at high dilution rates, chaos at intermediate dilution rates and stable limit cycles at low dilution rates.

However, there is still a lack of field evidence that limit cycle oscillations or chaotic behaviors surely occur in the natural seas and oceans. It seems unnatural to adopt limit cycle oscillations as a precondition of population variations. Thus, it is reasonable to conclude as follows. That is, random noise ubiquitously observed in the natural world is the source of persistent variations of inhomogeneous phytoplankton distributions, which plays a crucial role in patchiness formation together with turbulent stirring and mixing.

It is worth noting that random noise and limit cycles are not exclusive. A possibility cannot be denied that these two contribute together to patchiness formation. Indeed, further simulations show that the system containing both the noise process and the limit cycle oscillation can successfully produce realistic patchiness patterns. However, we can insist that the crucial factor is not limited cycles but noise processes that are responsible for phytoplankton patchiness in marine ecosystems.

From the technical point of view in computer simulations, appropriate incorporation of turbulence and noise

into the model is indispensable. The effects of these factors must be fully reflected in the simulations. The velocity field should be sufficiently energetic as the VF II (**Figure 2(b)**) rather than the VF I (**Figure 2(a)**). The white noise process should be slow enough as the WN II (**Figure 4(b)**) rather than the WN I (**Figure 4(a)**).

4.3. Extension to One-Component Model

In order to confirm robustness and applicability of the method, we finally attempt the simulation of patchiness formation using the different model. The exemplified mathematical model is a partial differential equation system with one variable, which is described as follows:

$$\frac{\partial P}{\partial t} = D\nabla^2 P - \nabla \cdot (VP) + I_p + \mu P \left(1 - \frac{P}{K}\right) - f_p \frac{P}{H_p + P} - m_p P + P\delta_p(x, y, t). \quad (11)$$

The reaction-advection-diffusion model **Eq.11** contains only one state variable P , which represents the phytoplankton density (the unit is g/m^2). The parameter K is the carrying capacity of the environment, and the meanings of the other parameters are the same as in the minimal NP models **Eqs.1** and **2** and **Eqs.7-9**. Moreover, the same velocity field (the VF II) and the same multiplicative white noise process (the WN II) as in **Figure 5** are employed in the simulation. It should be noted that limit cycles are impossible due to the use of the one-variable model. The system can give rise to only a convergence to the attractor, unless it diverges.

Figure 9 is an example of patchiness formation in the mathematical model **Eq.11**. The similar pattern formation with that in **Figure 5** proceeds, ensuring robustness and extensive applicability of the method described in this study.

5. CONCLUSIONS

1) Phytoplankton patchiness in marine ecosystems is essentially the physical phenomenon independent of

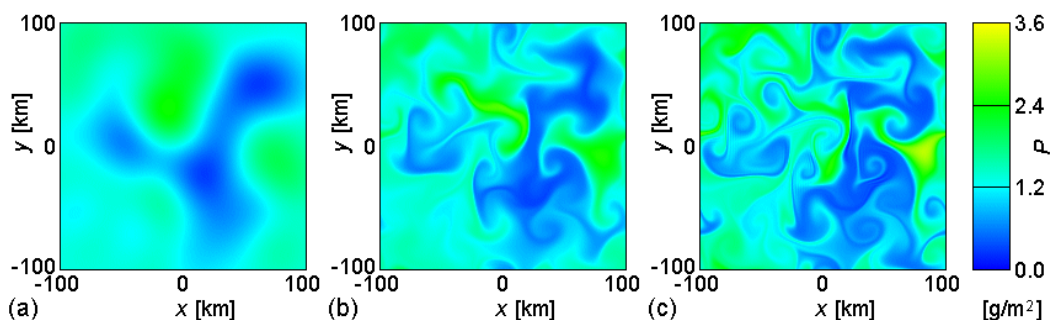


Figure 8. Spatiotemporal variation of phytoplankton distribution in minimal NP model **Eqs.7-9**. Without noise, the system shows a limit cycle oscillation for the parameter Set II in **Table 1**. In this case, patchiness formation is induced without fluctuations, supposing that the initial distribution is inhomogeneous. The VF II is employed. (a) $t = 0$ day, (b) $t = 6$ day, (c) $t = 12$ day.

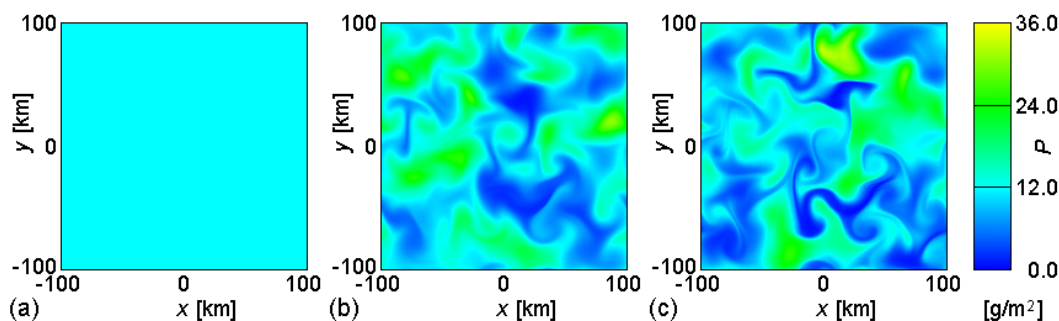


Figure 9. Spatiotemporal variation of phytoplankton distribution in mathematical model Eq.11. Without noise, the system shows a convergence to a stable equilibrium state for the following parameters: $I_p = 0.1 \text{ g} \cdot \text{m}^{-2} \cdot \text{day}^{-1}$, $\mu = 0.5 \text{ day}^{-1}$, $K = 20.0 \text{ g/m}^2$, $f_p = 1.6 \text{ g} \cdot \text{m}^{-2} \cdot \text{day}^{-1}$, $H_p = 2.4 \text{ g/m}^2$, $m_p = 0.1 \text{ day}^{-1}$. The units are altered to those of the two-dimensional model. The VF II and the WN II are employed. (a) $t = 0$ day, (b) $t = 6$ day, (c) $t = 12$ day.

each biological process. Turbulence and noise are two major factors that promote patchiness formation in oceanic environments. The pattern formation is guaranteed by persistent variations of the phytoplankton population. Stochastic noise is one of the most probable causes responsible for continuous variations. In addition, stirring and mixing by currents and eddies facilitate the creation of stretched and curled structures characteristic of phytoplankton patchiness.

2) Patchiness formation can be simulated in the spatially extended reaction-advection-diffusion system that properly integrates the turbulence field and the noise process. Sufficiently furious turbulence such as the VF II (Figure 2(b)) and slowly changing fluctuations such as the WN II (Figure 4(b)) are the key to reproduce realistic images of patchiness.

3) The simulations of patchiness formation can be performed by whatever model with the stable equilibrium state. Robustness in model simulations and applicability to various models could explain the universality of the phenomenon that is observed worldwide on Earth.

6. ACKNOWLEDGEMENTS

This study is supported by the Global COE Program “Global Eco-Risk Management from Asian View Points” by the Ministry of Education, Culture, Sports, Science and Technology, Japan.

REFERENCES

- [1] Martin, A.P. (2003) Phytoplankton patchiness: The role of lateral stirring and mixing. *Progress in Oceanography*, **57**(2), 125-174.
- [2] Medvinsky, A.B., Petrovskii, S.V., Tikhonova, I.A., Malchow, H. and Li, B.-L. (2002) Spatiotemporal complexity of plankton and fish dynamics. *SIAM Review*, **44**(3), 311-370.
- [3] Abraham, E.R. (1998) The generation of plankton patchiness by turbulent stirring. *Nature*, **391**(6667), 577-580.
- [4] Neufeld, Z., Haynes, P.H., Garçon, V. and Sudre, J. (2002) Ocean fertilization experiments may initiate a large scale phytoplankton bloom. *Geophysical Research Letters*, **29**(11), 1-4.
- [5] Tzella, A. and Haynes, P.H. (2007) Small-scale spatial structure in plankton distributions. *Biogeosciences*, **4**(2), 173-179.
- [6] Serizawa, H., Amemiya, T. and Itoh, K. (2008) Patchiness in a minimal nutrient-phytoplankton model. *Journal of Biosciences*, **33**(3), 391-403.
- [7] Dyke, P.P.G. and Robertson, T. (1985) The simulation of offshore turbulent dispersion using seeded eddies. *Applied Mathematical Modelling*, **9**(6), 429-433.
- [8] Serizawa, H., Amemiya, T. and Itoh, K. (2009) Noise-triggered regime shifts in a simple aquatic model. *Ecological Complexity*, **6**(3), 375-382.
- [9] Vainstein, M.H., Rubí, J.M. and Vilar, J.M.G. (2007) Stochastic population dynamics in turbulent fields. *The European Physical Journal-Special Topics*, **146**(1), 177-187.
- [10] Spagnolo, B., Valenti, D. and Fiasconaro, A. (2004) Noise in ecosystems: A short review. *Mathematical Biosciences and Engineering*, **1**(1), 185-211.
- [11] Provata, A., Sokolov, I.M. and Spagnolo, B. (2008) Editorial: Ecological complex systems. *The European Physical Journal B*, **65**(3), 307-314.
- [12] Guttal, V. and Jayaprakash, C. (2007) Impact of noise on bistable ecological systems. *Ecological Modelling*, **201**(3-4), 420-428.
- [13] Spagnolo, B., Fiasconaro, A. and Valenti, D. (2003) Noise induced phenomena in Lotka-Volterra systems. *Fluctuation and Noise Letters*, **3**(2), 177-185.
- [14] Serizawa, H., Amemiya, T. and Itoh, K. (2009) Patchiness and bistability in the comprehensive cyanobacterial model (CCM). *Ecological Modelling*, **220**(6), 764-773.
- [15] Okubo, A. (1971) Oceanic diffusion diagram. *Deep Sea Research and Oceanographic Abstracts*, **18**(8), 789-802.
- [16] Becks, L., Hilker, F.M., Malchow, H., Jürgens, K. and Arndt, H. (2005) Experimental demonstration of chaos in a microbial food web. *Nature*, **435**(30), 1226-1229.